UNIVERSITY OF BIRMINGHAM

University of Birmingham Research at Birmingham

Response of a molybdenum alloy to plasma nitriding

Zhang, Zhenxue; Li, Xiaoying; Dong, Hanshan

[Link to publication on Research at Birmingham portal](#)

Response of a molybdenum alloy to plasma nitriding

Zhenxue Zhang*

zhzhxue@yahoo.com

Xiaoying Li

Hanshan Dong

School of Metallurgy and Materials, University of Birmingham, Birmingham B15 2TT, UK

*Corresponding author.

Abstract

A molybdenum alloy (TZM: 0.50 wt% titanium, 0.08 wt% zirconium and 0.02 wt-% carbon with balanced molybdenum) was used to investigate its response to plasma nitriding in terms of layer formation and hardening at temperatures between 500 and 760 °C using various times. A thin hard nitride case plus a shallow diffusion zone was formed after plasma nitriding. The thickness of nitride layer increased with the treatment temperature and time. The nitrided surface of molybdenum alloy had a low coefficient of friction against the Al_2O_3 counterpart ball at ambient atmosphere and elevated temperatures, and the wear resistance of the surface was greatly improved. Molybdenum had a tendency to react with nitrogen to form a mixed nitride phases at the tested temperature range, and the TZM alloy had an activation energy of 330 kJ/mol.

Keywords: Plasma nitriding; Molybdenum; TZM; Friction; Al_2O_3

1 Introduction

When sintering high-strength materials at high temperatures, the major technical problems associated with traditional graphite dies in an electric-field-activated sintering technology (FAST) process, are their premature failure or short lifespan related to the low mechanical strength at elevated temperatures. Therefore tools (dies/punches) have to be made from superalloys, refractory metal alloys or even ceramics [1]. Titanium-Zirconium-Molybdenum (TZM) alloy is a great choice due to its stability and strength at elevated temperatures up to 1500 °C. In addition, TZM exhibits good thermal conductivity, high electrical conductivity and low coefficient of thermal expansion which make the materials resistant to thermal shock and cracking arisen when the tool surface experiencing cycles of rapid heating and cooling [2]. After sintering, the ceramic micro-parts need to be pushed to slide out the mould off-site or on-site depending on the production system setup and throughput. However, when the size of the tools and components is scaled down to millimetre-scale, soldering due to severe adhesion between the mould and the working material would occur and thus demoulding becomes a major challenge for Micro-FAST process.

In our earlier work on the sliding test between TZM and the ceramic materials (i.e. Al_2O_3 and Si_3N_4), it was found that the friction was high and had an adhesive character between TZM and Al_2O_3 counterpart ball which was not beneficial for a smooth demoulding, and thus some surface modifications or coatings were needed to improve the surface tribological properties [3]. Many attempts have been made to improve hot-working tools, such as surface welding, thermal spraying, electro-depositing, diffusion treatments and thermal chemical treatment like nitriding and carburising etc. Nagae and his colleagues nitrided pure molybdenum at 1100 °C in NH_3 gas for 16 h, and reported a molybdenum nitride surface layer formation which consists of a γ-Mo_2N outer layer and a β-Mo_2N inner layer [4]. However, Martinez's work found that no nitrogen absorption could happen under 800 °C in molybdenum and the reaction started between 800 and 1500 °C in a gas nitriding with forming gases (N_2+H_2). He attributed the slow nitriding of TZM to the existence of titanium, which is a strong nitride forming element [5]. It is widely known that the titanium alloys also need a high temperature (700-1000 °C) to be effectively nitrided [6]. High-temperature treatments generally led to recrystallization of the deformed molybdenum, and the forming gases, i.e. ammonia, embrittled the material [5], therefore the research on nitriding of molybdenum stalled for a long time. Recently, it was reported that molybdenum can be nitrided at a much lower temperature with the help of plasma. Jauberteau and his colleagues found that a deposited molybdenum layer could be nitrided at 600 °C in a gas mixture of argon, nitrogen and hydrogen by using an expanding microwave plasma reactor for an exposure time of 20 min [7]. They also claimed that Mo–N phases could be formed in molybdenum films even at a temperature as low as 400 °C, although the electron beam evaporation deposited molybdenum layer was very thin (400-600 nm) [8]. Their researches shed some light on plasma nitriding of molybdenum-based alloys at lower temperature, which has been widely reported to increase the surface hardness as well as the wear and corrosion resistance of hot-working tools [9]. Therefore it necessitates this research on plasma nitriding the molybdenum alloy at a lower temperature (<800 °C) to challenge the previous high temperature gas nitriding.

In the current research, DC plasma nitriding of TZM alloy between 500 and 760 °C was designed to investigate the response of molybdenum-based TZM alloy to the treatment temperature and time. The friction and wear behaviour of the nitrided and untreated TZM samples were compared by reciprocating sliding tests against Al_2O_3 at room temperature and unidirectional sliding at elevated temperature to simulate the demoulding of micro-ceramic sintering parts off-site or on-site.

2 Experimental

2.1 Design of the plasma nitriding processes

A molybdenum-based TZM alloy bar provided by *Edfagan Europe Inc.* was used in this study. It has a density of 10.22 g·cm^{-3} and chemical compositions of 0.50% titanium, 0.08% zirconium and 0.02% carbon (in wt.%) with balanced molybdenum. Coupons of Φ25 × 4.5 mm were sectioned and wet ground with SiC paper down to 1200 grit, followed by progressive polishing with 9, 6 and 1 μm diamond paste to generate a mirror-like finish.

Plasma nitriding was carried out in a 60 kW Klöchner DC plasma furnace at a pressure of 4 mbar. A DC voltage from 300 to 1000 V was applied between the sample (cathode) and the wall of the furnace (anode) during the process. The treatment temperature was measured with a thermocouple inserted in a hole in the jig. Temperature and duration increased gradually until a clear nitriding layer was observed (660/25). 13 batches of samples were plasma nitrided with a gas mixture of 25%N_2 and 75%H_2 at temperatures ranging from 500 to 760 °C for varied times. Detailed treatment conditions and the corresponding sample codes are listed in Table 1.

Table 1 Detailed plasma nitriding conditions and the corresponding sample codes.

alt-text: Table 1

Sample code	Temperature (°C)	Duration (hour)
500/5	500	5
550/10	550	10
600/20	600	20
660/25	660	25
720/12.5	720	12.5
720/25		25
720/37.5		37.5
720/50		50
720/62.5		62.5
720/75		75
760/8	760	8.33 (500 min)
760/16		16.67 (1000 min)
760/25		25 (1500 min)
Untreated	–	–

2.2 Characterization of the surface layers

The surface morphologies and microstructure of the plasma nitrided specimens were observed under scanning electron microscopy (JEOL 7000 SEM). The surface roughness was assessed by a XP-200 Plus Stylus 3D-profilometer. The phase constitution of the plasma nitrided layers was identified by X-ray diffraction (Philips X'pert X-Ray diffractometer) using a Cu-K$_\alpha$ radiation ($\lambda = 0.154$ nm). The chemical compositions of the layers were analysed using a glow discharge spectroscopy (GDS, LECO GDS-750 QDP), which allowed for continuous depth profiling for Mo and N. Metallographically prepared cross-section samples without etching were used for nano-hardness profiling using a nano-indenter (Micro Materials Ltd.) under a load of 20 mN. The surface micro-hardness was measured by a Vickers microhardness tester (Mitutoyo MVK-H1) under a load of 25 gf. Specimens were electrically etched in a phosphate solution for layer structure observation by JEOL 7000 SEM equipped with an Energy Dispersion X-ray (EDX) for the localised composition analysis. An X-ray photoelectron spectroscopy (XPS) was used to analyse the elemental valences on the nitrided surface.

2.3 Evaluation of the friction and wear properties of the surface layers

Friction and wear properties of the untreated and treated samples were assessed via a TE79 multi-axis tribology machine (Compend 2000 Version 2.3.1) in reciprocating mode at room temperature with a 8 mm in diameter Al_2O_3 ball as the counterpart under the

loads of 2, 5, 10 and 20 N respectively. The whole tribo-tester was enclosed in a chamber with transparent walls to avoid dust and air turbulence. The reciprocating sliding wear tests were conducted in air, in nitrogen by nitrogen purging, in distilled water and in simulated seawater containing 3% NaCl by filling the liquid into the container. The reciprocating sliding distance was set to 5 mm, the sliding speed was 10 mm/s, and the coefficient of friction (CoF) was recorded for 1000 cycles. Each reciprocating test was repeated 2–3 times until a stable curve was obtained, and only the positive side (one direction) was plotted as the value of CoF was symmetrical.

Unidirectional sliding wear tests were conducted using the CSM HT pin-on-disc tribo-tester under a load of 2 N with an Al_2O_3 ball of 6 mm in diameter at a unidirectional sliding speed of 10 cm/s for 5000 cycles at three different temperatures: room temperature (20 °C), 300 °C and 600 °C.

The wear tracks of the samples were measured utilising a XP-Plus Stylus Profilometer and the wear volumes were calculated accordingly. The morphology of the wear tracks was observed under SEM and the composition of the tracks was analysed by EDX.

3.3 Results

3.1.3.1 Surface morphology and roughness

The original shining metallic colour of the specimens was changed to varying bands of greyish after plasma nitriding treatments at 720 °C or under, and a typical one is shown in Figure 1a (720/25). The surface colour turned into dark grey with extended treatment time like 720/50 and 720/75. At 760 °C, the specimen surfaces were dark and grey and lack of metal lustre after 8.3-hour treatment and turned totally brownish after 25-hour treatment (Figure 1a right & Figure 1b).
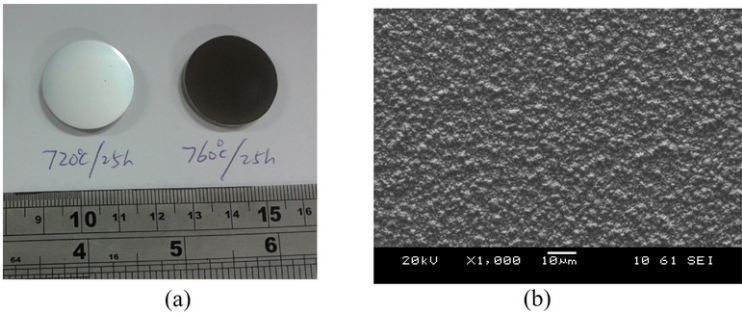

Figure 1. Fig. 1 Surface morphology changes after plasma nitriding: (a) as-PNed samples and (b) sample 760/25 surface under SEM.

alt-text: Fig. 1

The surface roughness was measured across a 0.5 mm length and the typical Ra value of a polished untreated TZM surface is about 0.01 μm. The Ra value was about 0.05 μm after plasma nitriding treatment of 660/25 and 720/25 as seen in Figure 2. The surface roughness was rapidly increased for treatment time longer than 37.5 h at 720 °C. When treated at 760 °C for 25 h (760/25), the surface became very rough with a Ra value of 0.1933. Generally, longer treatment time and higher treatment temperature led to a rougher surface.

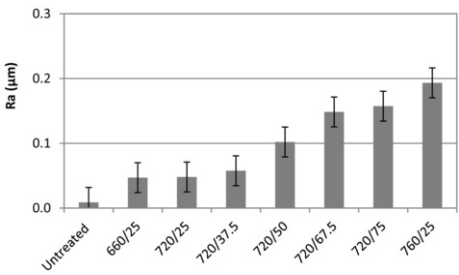Figure 2. Fig. 2 Surface roughness changes after different plasma nitriding treatments.

alt-text: Fig. 2

3.2.3.2 Surface layer structures

Cross-sectional SEM observations on all the nitrided samples revealed that a dense surface layer with some spikes along certain directions was formed (Figures 3a&b). There hardly any diffusion zone can be discerned under the hardened layer. For the samples

treated at the higher temperature (760/25), three layers in the nitride case can be distinguished under backscattering electron image as denoted by dashed lines in Figure 3c. The superficial layer is very thin and irregular, and the second and third layers are interlocked each other but with dark and light contrast respectively.
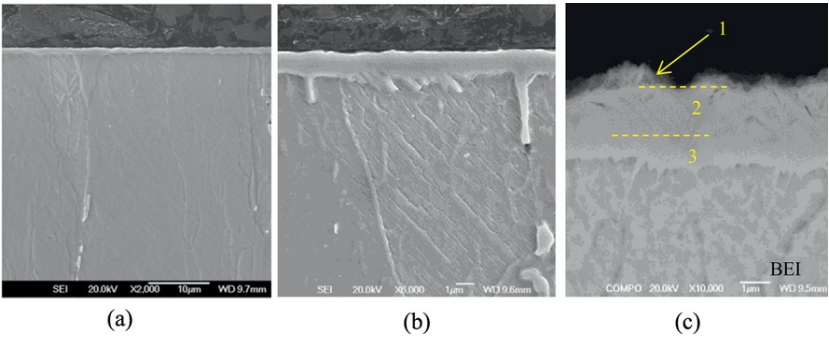

Figure 3.Fig. 3 Layer structures of plasma nitrided samples: (a) 660/25 (SEI image), (b) 720/25 (SEI image) and (c) 760/25 (BEI image).

alt-text: Fig. 3

3.3.3.3 Nitrogen distribution after plasma nitriding treatment

The typical elemental distribution trends of nitrogen of the samples treated at 720 °C against treatment time are shown in Figure 4. The depth of the nitrogen rich layer increased with the progress of the treatment time. For a 12.5-hour treatment, the nitrogen content decreases faster in the near surface area (up to 0.2 μm in depth) to an intermediate level (dashed line) and then decreased rapidly again from 0.5 to 0.75 μm to zero. For a 25-hour treatment (solid line), there are also three gradients of change for the nitrogen content: a very high gradient of descent in the near surface area up to 0.05 μm, a relatively low slope from 0.05–0.7 μm, and another accelerated decline from 0.7 to 1.6 μm to nearly nothing. For a 50-hour treatment (dotted line), apart from a sharp drop in the very near surface region, the nitrogen content comes down almost smoothly up to 3 μm. Oxygen has been detected in the near surface area which is also identified by EDX. For sample 760/25, nitrogen content peaks at the surface and decreases gradually in the near surface region to a relative level area to 2–3 μm deep, then there is an accelerated downward trend till zero at about 4 μm depth which represents the level in the substrate.
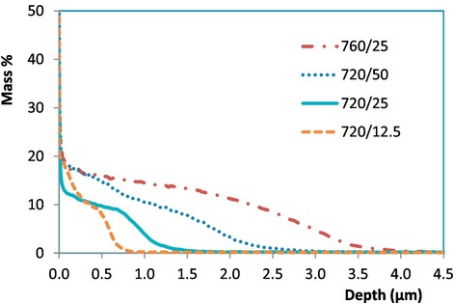

Figure 4.Fig. 4 Nitrogen distribution against the depth of sample 760/25 and samples treated at 720 °C for different times.

alt-text: Fig. 4

3.4.3.4 Surface phase constitutions and chemical information of the nitrided layers

The XRD patterns of the samples plasma nitrided at 660, 720 and 760 °C for 25 hoursh in a gas mixture of 25%N$_2$ + 75%H$_2$ and the as-received TZM sample are shown in Figure 5a. The typical bcc structure phase of molybdenum was identified for the untreated sample, as denoted by a cross mark in the XRD patterns. Compared with the untreated sample, the intensities of the bcc molybdenum peaks for all the plasma nitrided samples were reduced with the elevating temperature indicating an increased nitride layer thickness. Two nitride phases of MoN (ASTM01-089-4318) and Mo$_2$N (ASTM00-025-1366) were detected for all the nitrided samples. The major peaks of fcc γ-Mo$_2$N (circles) can be clearly identified for sample 660/25: (111), (200) and (220) corresponding to 2θ = 37.377°, 43.451° and 63.108° respectively (Figure 5a). In the meantime, peaks of hcp δ-MoN (triangles) can also be identified with the strongest peak of (022) corresponding to 2θ = 49.008°. For sample 720/25, the relative intensities of γ-Mo$_2$N phase especially (111) and (220) are stronger while the peaks of δ-MoN are reduced and the relative intensity is weakened (Figure 5a). However, for a short time treatment at 720 °C (720/12), a few more peaks of δ-MoN phase can be identified, such as (002) and (004) corresponding to 2θ = 31.89 and 66.656°. For a longer treatment (sample 720/75), apart from stronger γ-Mo$_2$N phase, more peaks of δ-MoN phase can be identified with strongest peaks of (022) and (002) at 2θ = 31.89 and 49.008° respectively. For treatments at 760 °C, with the increasing treatment time, the relative

intensities of δ-MoN phases were stronger and more peaks can be identified, however, three major γ-Mo$_2$N peaks are all weakened as seen in Figure 5b. There is no clear molybdenum oxide can be identified on the surface of the samples after short treatment (760/8 and 760/16), some weak peaks of oxides can be identified for sample 760/25.
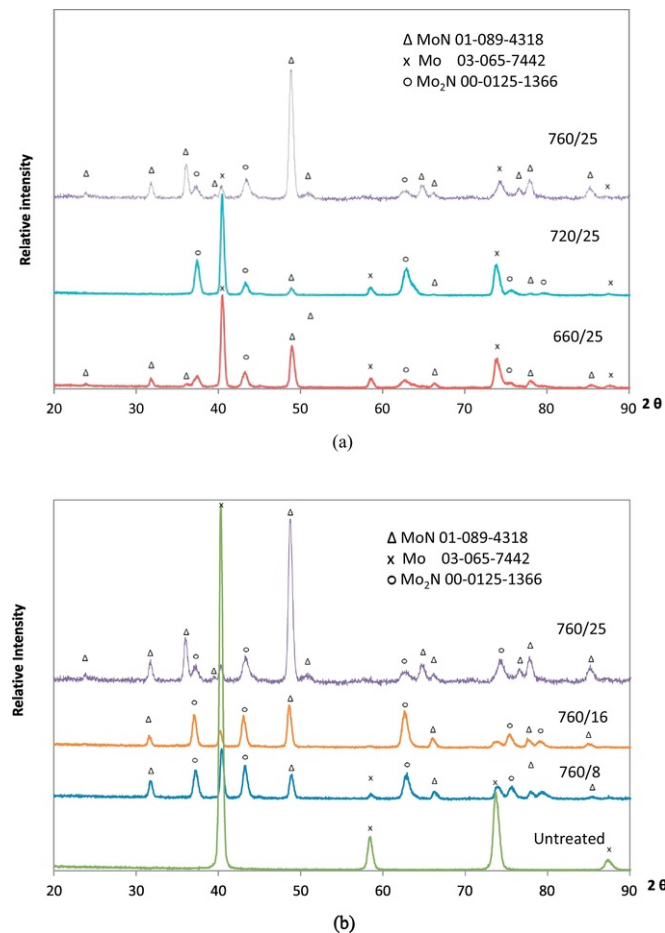

(a)

(b)

Figure 5.Fig. 5 Phase constituent changes with (a) temperature (25 h) and (b) treatment time (760 °C).

alt-text: Fig. 5

Figure 6 displays the X-ray photoelectron spectroscopy (XPS) characterization of plasma nitrided samples. The Mo 3d 5/2 peak is at 228.68 for the sample 720/25 which is close to the reported Mo^{2+} binding energy in the Mo$_2$N nitride [10], and it shifts slightly to 228.78 after the surface was polished away a very thin surface top layer (720/25P) indicating a stronger bond. The Mo 3d 5/2 peak shifts towards a higher binding energy 228.98 but less than the reported 230.0 for Mo^{4+} (MoN) with increasing treatment temperature and time (760/16 and 760/25P) suggesting high valence Mo species >2 or a mixture of valences. Peak of 231.88 and 231.98 (720/25 and 720/25P) is close to the report Mo^{5+} binding energy in the nitride, while peak of 232.08 (760/16) and 232.28 (760/25P) is more likely related to Mo^{6+} (Mo$_2$N$_3$). Peak of N1 s is 397.78 at the surface of 720/25 and increases slightly to 397.88 at a deeper layer (720/25P), it increases to 397.98 for 760/16 but decreases slightly to 397.18 for sample 760/25 even the very surface layer was polished away (760/25P) which suggesting the nitride was slightly oxidised. There was no peak in the binding energy area of titanium and zirconium which suggesting no titanium/zirconium nitride was formed at the surface and/or the deep layer of the nitride case of the abovementioned samples.
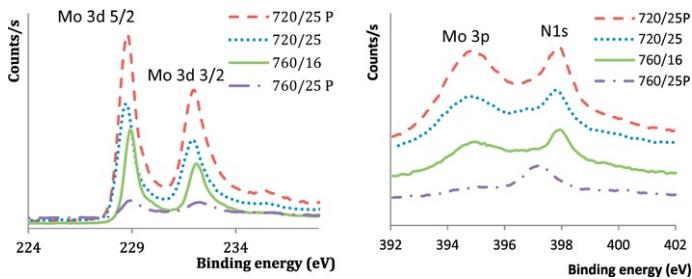
Figure 6Fig. 6 X-ray photoelectron spectroscopy (XPS) characterization of the surface of plasma nitrided samples (720/25P and 760/25P are the same samples of 720/25 and 760/25 with a slightly polished surface to remove the superficial layer).
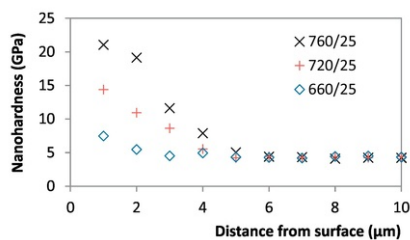
alt-text: Fig. 6

3.5.3.5 Hardness of the surface layer and depth profile

As shown in Figure 7a, for the same treatment time (25 h), the surface is harder with increasing treatment temperature (660, 720 and 760 °C). At the same treatment temperature (720 °C), the surface hardness increased with the extended treatment time. The nano-hardness plotted against the depth is shown in Figure 7b and a hard layer can be seen in all samples after plasma nitriding and the higher the treatment temperature, the harder the case and the near surface zone which is similar to the surface microhardness measurement as shown in Figure 4Fig. 7a.
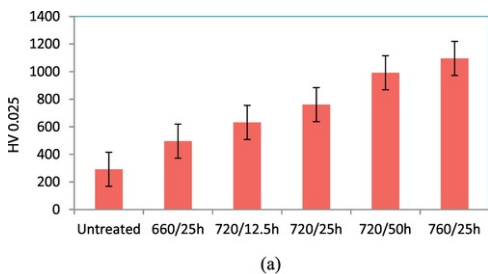
Figure 7.Fig. 7 (a) Surface micro-hardness changes; (b) Nano-hardness profile along the depth of the samples after nitriding treatment.

alt-text: Fig. 7

3.6.3.6 Tribological properties of the surface layers

Figure 8 shows the change of coefficient of friction (CoF) of the plasma nitrided TZM sample (720/25) against moving cycles with Al_2O_3 counterpart ball at different loads (5 N, 10 N and 20 N) in the air compared with the untreated sample (5 N). Under a load of 5 N with an Al_2O_3 counterpart ball, the calculated maximum Hertzian contact pressure was about 1300 MPa for the untreated TZM sample. As can be seen in Figure 8, the CoF of the untreated TZM sample was high and unstable at the beginning of the test and then gradually reduced to about 0.45 at the end of the test. For the plasma treated sample (720/25), under a load of 5 N, the calculated maximum Hertzian contact pressure increased to more than >1400 MPa due to a higher Young's modulus and lower Poisson ratio of molybdenum nitrides. The CoF revealed a very low value of 0.08 at the beginning and increased steadily to around 0.25 after about 150 cycles (Figure 8). When 10 N and 20 N loads were applied, the maximum Hertzian contact pressure increased to more than >2000 MPa, and the CoFs increased at a very slow pace to about 0.30 at the end of the test. Overall the CoF was under 0.3 which was much lower than the value for the untreated TZM sample. It was found that the change of coefficient of friction (CoF) showed a similar trend for other

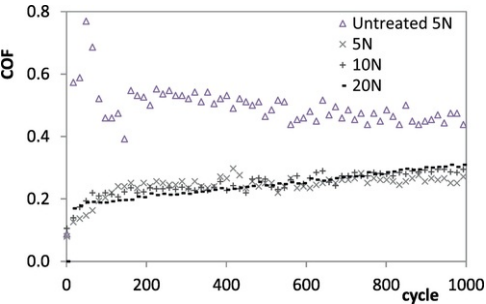plasma nitrided samples when tested under a load of 2 N.

Fig. 8 Coefficient of friction for untreated and PN treated (720/25) samples measured under different loads.

alt-text: Fig. 8

Post friction test wear tracks were plotted in 2-D profiles as shown in Figure. 9. A clear, deep concave wear track was worn on untreated sample by an Al_2O_3 counterpart ball under a load of 5 N. For the plasma nitrided sample (720/25), the wear tracks were very shallow and quite smooth even under a load of 20 N. SEM observations revealed that some flaky pieces were peeled off and then smeared on the bottom of the wear track for the untreated samples and patch of debris was stuck on the wear surface of the Al_2O_3 ball [3] (Figure. 8 right side inset picture). However, this flaky feature was not observed for the track of plasma nitrided sample (720/25) tested under the same load and higher loads (10 N and 20 N). Some transverse cracks were observed at the bottom of the track tested under 20 N and minor scratch marks can be seen on the Al_2O_3 counterpart ball (Figure. 9 left side inset picture). EDX analysis at different spots of the wear tracks revealed that the light and the dark bit in the cracked area was high in oxygen and nitrogen indicating the area was partially oxidised during tribo-test.
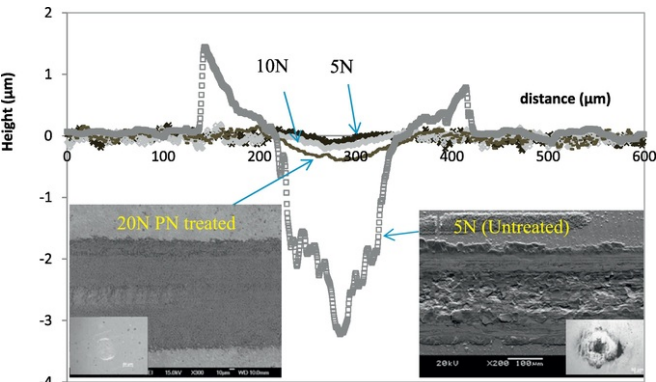

Fig. 9 Wear tracks for the untreated and PN treated (720/25) samples at different loads and the SEM images of the wear track of untreated sample under a load of 5 N and the scar on the Al_2O_3 ball, and the wear track of the PN treated sample (720/25) under a load of 20 N and the scar on the Al_2O_3 ball.

alt-text: Fig. 9

Unidirectional pin-on-disc friction tests at elevated temperatures of untreated and plasma nitrided samples are compared in Figure. 10. When tested at 300 °C, the CoF of untreated sample increased gradually from 0.65 to above 0.9 at 2400 cycles until the end of the test (Figure. 10). The initial frictions were low for the PN treated samples, and the CoF increased rapidly to 0.57 at cycle 333, and it then decreased slowly to 0.48 at cycle 1067 and climbed up steadily and slowly to 0.67 till the end of the tribo-test. The CoF changes against the cycle of the other plasma nitrided samples showed a similar trend.
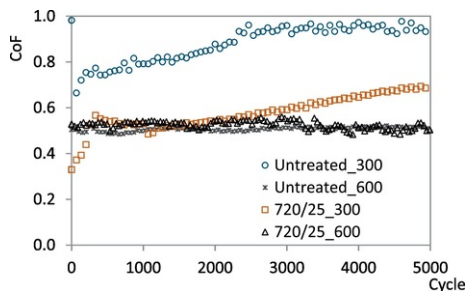
Figure 10. Fig. 10 Coefficient of friction comparison of untreated and PN treated (720/25) samples under elevated temperatures of 300 °C and 600 °C.

alt-text: Fig. 10

Interestingly, when tested at 600 °C, apart from the short running-in process, the CoFs of PN treated and untreated samples were all fluctuating at a relatively low value of 0.5 during the whole tribo-test cycles (Figure. 10). SEM observations on the tested track revealed that the surface of the sample were all oxidised at 600 °C due to the test rig run in the ambient environment. The wear rate of plasma treated sample at 600 °C was calculated, and it was about 0.0452 × 10^{-3} mm^3/m which was slightly higher than that of the untreated sample of 0.0258 mm^3/m as reported earlier [3].

4.4 Discussion

A rather thin nitride case with a limited diffusion zone was formed on the surface of the molybdenum-based TZM after plasma nitriding in a mixture of 25% N$_2$ and 75% H$_2$ in comparison with other materials like stainless steel and the treatment temperature is at 660 °C and above [11,12]. This is similar to the plasma nitriding of titanium alloys which is typically carried out in the temperature range of 700–1100 °C for 6–80 hoursh in a nitrogen-containing medium [6].

4.1.4.1 The nitriding mechanism of molybdenum-based TZM alloy

The thickness of the nitride layer was measured under SEM in correlation to the nitrogen profiles measured by GDOES. For a fixed treatment time of 25 hoursh, the thickness of nitride layer increased with the elevated temperatures. For a fixed treatment temperature of 720 or 760 °C, nitrided layer grew steadily with the treatment time. The square thickness increases nearly linearly with the treatment time as shown in Figure. 11. Based on this, the activation energy for the nitrogen diffusion in this molybdenum-based TZM alloy can be calculated as 330 kJ/mol. However, it has been reported that the activation energy is between 100 and 200 kJ/mol for outgassing of nitrogen in a nitrogen saturated molybdenum at temperatures between 1050 and 1950 °C in an ultrahigh vacuum [13]. This means that it needs a high energy to activate the nitriding of TZM alloy.
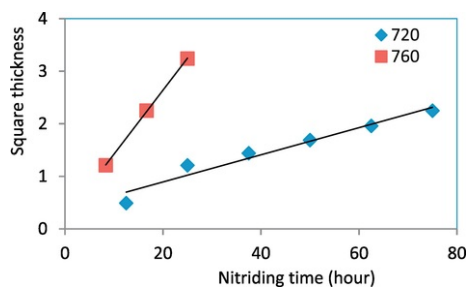

Figure 11. Fig. 11 Square thickness against nitriding time at 720 °C and 760 °C.

alt-text: Fig. 11

Direct reactions of the metal with nitrogen gas employ very high temperatures to cleave the strong N— N triple bond. Earlier reports suggested that there was hardly any nitrogen absorption for molybdenum alloys under 800 °C in a gas nitriding [4,5]. The use of NH$_3$ instead of N$_2$ as reactive gas is not easy to control and often leads to a mixture of phases. Moreover, the decomposition of NH$_3$ is endothermic but it can be replaced by N$_2$–H$_2$ gas mixtures, which circumvent the problem of heat transfer [14]. Some researchers used different approaches like an expanding microwave plasma reactor to form a Mo— N compound with defects at 600 °C or under in a gas mixture of Ar–25%N$_2$–30%H$_2$ [7,8].

In the plasma nitriding process, nitrogen ions and radicals such as N$^+$, N^{2+}, as well as fast neutral nitrogen molecules play a significant role in nitrogen transfer, and the presence of hydrogen in the nitriding medium results in the formation of H$^+$, NH$^+$, and NH^{2+} radicals that have a catalytic effect on nitriding kinetics through increased diffusion of nitrogen into the molybdenum alloy by reducing the remaining passive oxide and carbide layers. This occurs either by generating active nitrogen atoms on the cathodic part surface or by attaching to atoms sputtered from the surface and redeposited back on the cathode in the form of nitrides [15]. Given plenty of energy, i.e., at the temperature of 600 °C or above, molybdenum would react with the activated nitrogen ions to form molybdenum nitrides. According to Mo-N phase diagram, β-Mo$_2$N is easy to form at a lower temperature (i.e. 400 °C), and γ-Mo$_2$N is more likely to form at higher temperature [16]. As seen in Figure 4, the nitrogen content at the interface of nitride case and substrate i.e. reaction front is higher than that in stoichiometric Mo$_2$N (6.82 mass%), which suggesting γ-Mo$_2$N (JCPD 00-025-1366) would be easier to form initially as shown in Figure 5. With further nitrogen was taken into the Mo$_2$N layer, the N/Mo ratio can be as high as 1/3 (Figure 4) which exceeds the nitrogen content in MoN (12.74 mass %), thus MoN was likely to be formed in the near surface region. XPS analysis suggested that Mo$_2$N$_3$ can also be formed (Figure 6). Therefore, there might be more MoN/Mo$_2$N$_3$ formed in the near-surface region (higher nitrogen content) and more Mo$_2$N formed near to the interface (lower nitrogen content) which is reflected from the nitrogen distribution as seen in Figure 4a&b. This is in agreement with Kazmanli's report that increasing the nitrogen pressure causes a transition from Mo to Mo$_2$N and then MoN [17].

When the treatment temperature was raised to 760 °C, three sub-layers (760/25) can be distinguished in the nitride case under backscattering electron image as seen in Figure 3c. The top superficial layer is supposed to be oxide layer as high oxygen content can also be traced in GDOES analysis. The N 1s peak decreases slightly in the XPS analysis for sample 760/25 even the very surface layer was polished (760/25P) which indicating the molybdenum nitrides was slightly oxidised (Figure 6). However, this oxide layer is hardly discernible for samples treated at a lower temperature (720/660 °C). The sublayer under oxide is of high nitrogen concentration (Figure 4a) which is deemed as MoN. Face centred cubic δ-MoN phase has been identified in all the samples but the relative intensity increases with temperature and treatment time increase (Figure 5), which suggests increased thickness of the nitride layer. The sublayer interfaced with the substrate is believed to be Mo$_2$N as nitrogen content decreased. A sharp drop of nano-hardness across the interface in Figure 7b and no clear visible diffusion zone under the nitride layer (Figure 3) suggests that a shallow and limited diffusion zone was formed as the nitrogen has a very low solubility in molybdenum and its alloy (1.08 atom% at room temperature) [16]. It is well-known that diffusion of nitrogen is much faster along grain boundaries than through the bulk grains i.e. short-circuit diffusion. Hence, nitrogen would preferentially diffuse along grain boundaries therefore some nitrides can be found in a much deeper depth as indicated in Figure 3. Once the dense and compact nitride layer was formed, it would form a barrier for nitrogen intake and diffusion thus slowed the growth of the nitride layer, and this has been found in the plasma nitriding of other metallic materials.

4.2 Low friction of nitrided TZM surface for a long life tool

The molybdenum nitride phases have different lattice structures and parameters, which affect the properties of the coating. Within the Mo–N system, the stoichiometric hexagonal compound δ-MoN is a high-hardness material with very low compressibility [18]. Kazmanli et al. [17] reported that MoN (hexagonal) coatings exhibited a greater hardness (5000 kg/mm^2) compared with Mo$_2$N (f.c.c.) coating (3500 kg/mm^2) which is in agreement with Jehn's and Khojer's findings [19–20]. In this research, the thicker MoN increased with treatment temperature and time was more likely responsible for the increased surface hardness and the nitride case. It is reported that increasing the annealing temperature causes an increase of surface roughness which is in agreement with current finding as shown in Figure 2 [20]. Clearly, the dense and compact nitride layer with higher hardness is responsible for the reduction of the coefficient of friction and wear volume (Figure 8-10). A similar CoF of 0.2 for an arc-PVD deposited Mo-N coating on HSS against an alumina counterpart ball under a load of 7 N was reported by Urgen et al. [21]. The wear of Al$_2$O$_3$ against untreated TZM is of typical adhesive feature but is of abrasive wear when against plasma nitride TZM sample. The CoFs of the plasma nitrided sample are lower at 300 °C than that of the untreated sample but they are quite similar at 600 °C. Molybdenum oxidises at a temperature above 400 °C, and MoO$_3$ is an oxygen deficient phase known as Magnéli phase which has lubrication effect at elevated temperatures [22]. Molybdenum nitrides can also be oxidised at 600 °C, and the lubricated oxides give the plasma nitrided surface a similar friction curve as that of untreated sample. A vacuum or inert gas protected environment is needed to further assess the tribological properties of plasma nitrided sample at elevated temperature.

TZM was proposed to be used as tool material in electric-field-activated sintering of ceramics like Al$_2$O$_3$ etc. The relatively low coefficient of friction of the nitrided surface enables the demoulding of the sintering part off-site (room temperatrue) or on-site (elevated temperatures). Currently, we have used the plasma nitrided TZM punches (Figure 12) in the sintering of Al$_2$O$_3$ micro-parts which has shown a much-extended life and acceptable low friction in demoulding over a peer graphite punch at room temperature.
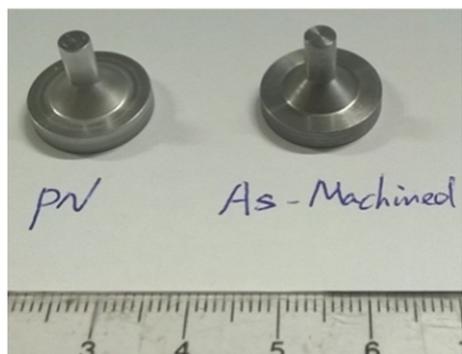

Fig. 12 As machined and plasma nitrided TZM punches.

5 Conclusions

The response of molybdenum-based TZM in terms of layer formation and hardening to plasma nitriding at temperatures between 500 and 760 °C has been investigated. After plasma nitriding, a thin nitride case composing of mixed phases of Mo_2N and MoN plus a shallow diffusion zone was formed.

- The thickness of plasma nitride layer increased with the treatment temperature and time, and the TZM alloy has an activation energy of 330 kJ/mol in the treatment temperature range.

- Molybdenum has a tendency to react with nitrogen to first form γ-Mo_2N and then δ-MoN during the plasma nitriding treatment.

- The surface hardness of molybdenum-based TZM alloy was significantly increased after plasma nitriding treatment which is also related to the treatment temperature and time.

- The coefficient of friction of the molybdenum-based TZM against Al_2O_3 ball was reduced significantly due to the formation of a thin nitride layer regardless of the loads and medium used. The wear resistance of the plasma nitriding treated surface was greatly improved. A lower CoF of plasma nitrided TZM against Al_2O_3 ball was also observed at elevated temperature.

Acknowledgement

References

[1] S.P. Chakraborty, Studies on the development of TZM alloy by aluminothermic coreduction process and formation of protective coating over the alloy by plasma spray technique, *Int. J. Refract. Met. Hard Mater.* **29**, 2011, 623–630, https://doi.org/10.1016/j.ijrmhm.2011.04.010.

[2] J.A. Shields, (title of the reference should be added: Applications of molybdenum metal and its alloys,)International Molybdenum Association (IMOA), www.imoa.info, 2013.

[3] Z. Zhang, X. Li, E. Almandoz, G.G. Fuentes and H. Dong, Titanium-Zirconium-Molybdenum (TZM) alloy against Al2O3 and Si3N4 balls under several environments and temperatures, *Tribol. Int.* **110**, 2017, 348–357, https://doi.org/10.1016/j.triboint.2016.10.049.

[4] M. Nagae, T. Yoshio, Y. Takemoto and J. Takada, Microstructure of a molybdenum nitride layer formed by nitriding molybdenum metal, *J. Am. Ceram. Soc.* **84**, 2001, 1175–1177.

[5] H.-P. Martinz and K. Prandini, The carburization and nitriding of molybdenum and TZM, *Int. J. Refract. Met. Hard Mater.* **12**, 1993-1994, 179–186.

[6] A. Edrisy and K. Farokhzadeh, Plasma Nitriding of Titanium Alloys in Plasma Science and Technology - Progress in Physical States and Chemical Reactions (ed Tetsu Mieno) Ch. 3, 2016, InTech, 63–105.

[7] I. Jauberteau, et al., Investigations on a nitriding process of molybdenum thin films exposed to (Ar–N2–H2) expanding microwave plasma, *Surf. Coat. Technol.* **203**, 2009, 1127–1132.

[8] I. Jauberteau, et al., Expanding microwave plasma process for thin molybdenum films nitriding: nitrogen diffusion and structure investigations, *Surf. Coat. Technol.* **205**, 2011, S271–S274.

[9] S. Ma, K. Xu, W. Jie, et al., *Surf. Coat. Technol.* **191**, 2005, 201–205, (please add the title of the reference: Plasma nitrided and TiCN coated AISI H13 steel by pulsed dc PECVD and its application for hot-working dies) https://doi.org/10.1016/j.surfcoat.2004.03.048.

[10] Z.B.Z. Wei, P. Grange and B. Delmon, XPS and XRD studies of fresh and sulfided Mo2N, *Appl. Surf. Sci.* **135**, 1998.

[11] K. Lin, X. Li, Y. Sun, X. Luo and H. Dong, Active screen plasma nitriding of 316 stainless steel for the application of bipolar plates in proton exchange membrane fuel cells, *Int. J. Hydrog. Energy* **39**, 2014, 21470–21479, https://doi.org/10.1016/j.ijhydene.2014.04.102.

[12] Z. Zhang, X. Li and H. Dong, Plasma-nitriding and characterization of FeAl40 iron aluminide, *Acta Mater.* **86**, 2015, 341–351, https://doi.org/10.1016/j.actamat.2014.11.044.

[13] D.E. Weaver, The Diffusivity and Solubility of Nitrogen in Molybdenum and the Trapping of Nitrogen by Carbon in Molybdenum PhD Thesis, 1972, University of California.

[14] I. Jauberteau, et al., Molybdenum nitride films: crystal structures, synthesis, mechanical, electrical and some other properties, *CoatingsTech* **5**, 2015, 656–687, https://doi.org/10.3390/coatings5040656.

[15] E. Roliński, A. Konieczny and G. Sharp, Influence of nitriding mechanisms on surface roughness of plasma and gas nitrided/nitrocarburized gray cast iron, *Heat treating progress* **3/4**, 2007, 39–46.

[16] H. Jehn and P. Ettmayer, The molybdenum-nitrogen phase diagram, *J. Less-Common Met.* **58**, 1978, 85–98.

[17] ~~M. K.~~ M.K. Kazmanli, M. Ürgen and ~~A. F.~~ A.F. Cakir, Effect of nitrogen pressure, bias voltage and substrate temperature on the phase structure of Mo–N coatings produced by cathodic arc PVD, *Surf. Coat. Technol.* **167**, 2003, 77–82, https://doi.org/10.1016/S0257-8972(02)00866-6.

[18] ~~C. L.~~ C.L. Bull, et al., Crystal structure and high-pressure properties of γ-Mo2N determined by neutron powder diffraction and X-ray diffraction, *J. Solid State Chem.* **179**, 2006, 1762–1767, https://doi.org/10.1016/j.jssc.2006.03.011.

[19] H. Jehn, W. Kurtz, D. Schneider, U. Trobisch and J. Wagner, In: Hartmut Katscher, Wolfgang Kurtz and Friedrich Schröder, (Eds.), *Gmelin Handbook of Inorganic Chemistry Vol. Supplement B5,* 1989, Springer.

[20] K. Khojier, ~~M. R. K.~~ M.R.K. Mehr and H. Savaloni, Annealing temperature effect on the mechanical and tribological properties of molybdenum nitride thin films, *Journal of Nanostructure in Chemistry* **3**, 2013, 5, https://doi.org/10.1186/2193-8865-3-5.

[21] M. Ürgen, et al., Characterization of molybdenum nitride coatings produced by arc-PVD technique, *Surf. Coat. Technol.* **94**, 1997, 501–506, https://doi.org/10.1016/S0257-8972(97)00432-5.

[22] W. Gulbiński, T. Suszko, W. Sienicki and B. Warcholiński, Tribological properties of silver- and copper-doped transition metal oxide coatings, *Wear* **254**, 2003, 129–135, https://doi.org/10.1016/S0043-1648(02)00292-2.

Highlights

- TZM Molybdenum alloy can be effectively plasma nitrided at temperatures between 660 and 760 °C.

- The thin nitrided surface has a low coefficient of friction of about 0.2 at ambient atmosphere against the Al_2O_3 ball.

- Low friction of nitrided TZM surface is beneficial in the demoulding of electric-field-activated sintering of ceramics.

Queries and Answers

Query:

Your article is registered as a regular item and is being processed for inclusion in a regular issue of the journal. If this is NOT correct and your article belongs to a Special Issue/Collection please contact d.joseph@elsevier.com immediately prior to returning your corrections.

Answer: Yes

Query:

Please confirm that given names and surnames have been identified correctly and are presented in the desired order, and please carefully verify the spelling of all authors' names.

Answer: Yes

Query:

The author names have been tagged as given names and surnames (surnames are highlighted in teal color). Please confirm if they have been identified correctly.

Answer: Yes

Query:

An e-mail address is mandatory for corresponding authors; however, private e-mail addresses (e.g., gmail, hotmail, yahoo) should not be included. Please check if an alternative academic/institutional e-mail address can be provided for the corresponding author/s.

Answer: z.zhang.1@bham.ac.uk

Query:

Duplicate Fig. 11 was renumbered to Fig. 12 including the citation. Please check and confirm if the action done is correct.

Answer: Yes